

## Nature of Metal–Metal Interactions in Systems with Bridging Ligands. 2. Electronic and Molecular Structure of the Cyclopentadienylnitrosylcobalt Dimer and Related Molecules

Arthur A. Low<sup>†</sup> and Michael B. Hall\*

Department of Chemistry, Texas A&M University, College Station, Texas 77843-3255

Received February 4, 1993

*Ab initio* calculations on  $(\eta^5\text{-C}_5\text{H}_5)_2\text{Co}_2(\mu\text{-NO})_2$  show that the singlet ground state possesses a bent, "butterfly" core ( $\text{Co}_2\text{N}_2$ ) in contrast to the published X-ray structure but in agreement with both the solution and solid-state IR measurements. This bent, singlet ground state lies nearly 100 kJ mol<sup>-1</sup> below the planar singlet or triplet states, which are nearly degenerate. Our results resolve the discrepancy between other recent theoretical results which predict a low-lying triplet state for the planar structure and the magnetic susceptibility measurements which prove that the molecule is diamagnetic with no low-lying paramagnetic states. Further evidence that our predicted structure is correct comes from parallel calculations, reported here, that correctly predict the structure of the related  $(\eta^5\text{-C}_5\text{H}_5)_2\text{Fe}_2(\mu\text{-NO})_2$ ,  $(\eta^5\text{-C}_5\text{H}_5)_2\text{Co}_2(\mu\text{-CO})_2$ , and  $(\eta^5\text{-C}_5\text{H}_5)_2\text{Ni}_2(\mu\text{-CO})_2$  molecules. Detailed topological analysis of the electron density of  $(\eta^5\text{-C}_5\text{H}_5)_2\text{Co}_2(\mu\text{-NO})_2$  shows that at certain geometries and levels of electron correlation there exists a Co–Co bond but at other geometries and levels of electron correlation the Co–Co bond critical point vanishes, to be replaced by a  $\text{Co}_2\text{N}_2$  ring critical point. Thus, we must conclude that, like  $\text{Co}_2(\text{CO})_8$ , the Co–Co interaction is below the region of change from having to not having a bond. Orbital and deformation density analyses of the bent dimer support the traditional view of a Co–Co single bond, albeit a weak one. A redetermination of the structure of  $(\eta^5\text{-C}_5\text{H}_5)_2\text{Co}_2(\mu\text{-NO})_2$  might result in a different Co–Co bond length, which would help resolve the nature of the Co–Co interaction and finally resolve the longstanding dilemma of the lack of variation in Co–Co bond distances with bond order as the bridging ligands are changed from nitrosyl to carbonyl.

### Introduction

The nature of the interaction between the metals in dinuclear transition metal complexes containing bridging  $\pi$ -acid ligands has been the subject of intense experimental and theoretical research. An interesting class of these dinuclear transition metal complexes are those with the general formula  $\text{Cp}_2\text{M}_2(\mu\text{-AO})_2$  ( $\text{Cp} = \eta^5\text{-C}_5\text{H}_5$  or any methylated derivative;  $\text{M} = \text{Fe}, \text{Co}, \text{Ni}$  or  $\text{Ru}$ ;  $\text{A} = \text{C}$  or  $\text{N}$ ).<sup>1</sup> These complexes are simultaneously similar to one another structurally and dissimilar electronically.

If the effective atomic number rule is strictly followed, the complexes range from those that contain a formal double bond between the metals, as in  $(\eta^5\text{-C}_5\text{H}_5)_2\text{Fe}_2(\mu\text{-NO})_2^2$  and  $(\eta^5\text{-C}_5\text{-Me}_3)_2\text{Co}_2(\mu\text{-CO})_2^3$  to those that contain a formal single bond between the metals, as in  $(\eta^5\text{-C}_5\text{H}_5)_2\text{Ni}_2(\mu\text{-CO})_2^4$  and  $(\eta^5\text{-C}_5\text{H}_5)_2\text{Co}_2(\mu\text{-NO})_2^5$ . In fact, with the appropriate choice of bridging ligand, there are reported dinuclear cobalt complexes which have formal bond of 1.5, as in  $(\eta^5\text{-C}_5\text{H}_5)_2\text{Co}_2(\mu\text{-CO})(\mu\text{-NO})^5$ . Solely on the basis of this electron counting procedure, it might be expected that a wide range of metal–metal separations would be observed in these complexes. However, the variation is surprisingly small. For example, in  $(\eta^5\text{-C}_5\text{Me}_3)_2\text{Co}_2(\mu\text{-CO})_2$  the separation between the cobalts is 2.338 Å,<sup>6</sup> in  $(\eta^5\text{-C}_5\text{H}_5)_2\text{Co}_2(\mu\text{-CO})(\mu\text{-NO})$  it is slightly longer at 2.370 Å,<sup>5</sup> and in  $(\eta^5\text{-C}_5\text{H}_5)_2\text{Co}_2(\mu\text{-NO})_2$  it is 2.372 Å.<sup>5</sup> In fact, there is little variation in the metal–metal separation in this entire family of compounds with a minimum separation of 2.326 Å for  $(\eta^5\text{-C}_5\text{H}_5)_2\text{Fe}_2(\mu\text{-NO})_2^2$  to a maximum of 2.390 Å for  $(\eta^5\text{-C}_5\text{H}_4\text{Me})_2\text{Ni}_2(\mu\text{-CO})_2^3$  a difference of only 0.064 Å. The lack of variance in the metal–metal separation between the dinuclear cobalt complexes led to

the conclusion by Bernal et al.<sup>5</sup> that "the successive increase in bond order predicted by the EAN rule is not observed."

The major structural difference among these complexes is whether the  $\text{M}_2(\mu\text{-AO})_2$  core adopts a planar or bent geometry (see Figure 1). For some of the complexes, especially those with the higher formal bond orders, the  $\text{M}_2(\mu\text{-AO})_2$  core is planar in a plane with the terminal cyclopentadienyl ligands lying in a plane perpendicular to the first plane and parallel to each other. Other complexes, especially those with the lower bond orders, adopt a bent geometry in which the metals and bridging ligands form a "butterfly-like" structure with dihedral angles (denoted as  $\phi$ ) between the two planes which contain the  $\text{M}_2(\mu\text{-AO})_2$  core ranging from 176 to 130°. In addition, the cyclopentadienyl ligand "tilts" with respect to their positions in the planar complex so that the cyclopentadienyl ligand moves away from the bridging ligands.

For some of the dinuclear complexes, the energy difference between a planar and bent structure seems to be quite small and the complex adopts a planar structure in one phase and a bent structure in another phase. A simple method of determining whether a complex adopts a planar or bent structure is to find the number of bridging ligand stretching frequencies ( $\nu_{\text{AO}}$ 's) in the complex's infrared (IR) spectrum. A complex with a bent geometry will possess two  $\nu_{\text{AO}}$ 's in its spectrum, whereas a planar geometry will have only one  $\nu_{\text{AO}}$  in its spectrum because the symmetric  $\nu_{\text{AO}}$  is IR-inactive.

Examination of the number of  $\nu_{\text{AO}}$  in the IR spectra of these complexes shows the floppiness of some of these dinuclear complexes. For example, the complex  $[(\eta^5\text{-C}_5\text{Me}_3)_2\text{Co}_2(\mu\text{-CO})_2]^-$  possesses only one  $\nu_{\text{CO}}$  in its solution-state (THF) IR spectrum indicative of a planar structure, but the solid-state (Nujol) spectrum of the same anion shows two  $\nu_{\text{CO}}$ 's, indicative of the bent geometry the anion assumes in the solid state as verified by its crystal structure analysis.<sup>6</sup> There are also examples of the opposite behavior. For example,  $(\eta^5\text{-C}_5\text{H}_5)_2\text{Ni}_2(\mu\text{-CO})_2$  adopts a planar geometry in the solid state as shown by X-ray crystallography and the appearance of only one  $\nu_{\text{CO}}$  in its solid-

<sup>†</sup> Present address: Department of Physical Sciences, Tarleton Station, Tarleton State University, Stephenville, TX 76402.

- (1) For a detailed list see: Bottomley, F. *Inorg. Chem.* **1983**, *22*, 2656.
- (2) Brunner, H. *J. Organomet. Chem.* **1968**, *14*, 173.
- (3) Bailey, W. I.; Collins, D. M.; Cotton, F. A.; Baldwin, J. C.; Kaska, W. C. *J. Organomet. Chem.* **1989**, *165*, 373.
- (4) Byers, L. F.; Dahl, L. F. *Inorg. Chem.* **1980**, *19*, 680.
- (5) Bernal, I.; Korp, J. D.; Reisner, G. M.; Herrmann, W. A. *J. Organomet. Chem.* **1977**, *139*, 321.
- (6) Cirjak, L. M.; Ginsburg, R. E.; Dahl, L. F. *Inorg. Chem.* **1982**, *21*, 940.

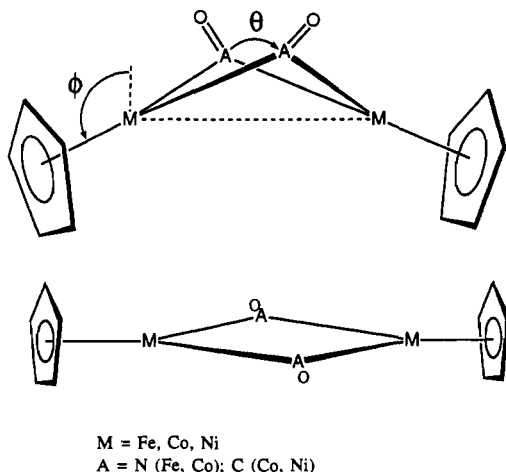


**Figure 1.** Two basic types of geometries adopted by complexes with the general formula  $\text{Cp}_2\text{M}_2(\mu\text{-AO})_2$  ( $\text{M} = \text{Fe, Co, Ni, Ru}$ ;  $\text{A} = \text{C, N}$ ). The bent geometry is characterized by a cyclopentadienyl "tilt" angle,  $\phi$ , and a  $\text{M}_2(\mu\text{-AO})_2$  "puckering" angle,  $\theta$ .

state infrared spectrum, but the solution-state IR spectrum of this Ni complex possesses two  $\nu_{\text{CO}}$ 's indicative of a bent geometry.<sup>3</sup>

One of the more interesting complexes,  $(\eta^5\text{-C}_5\text{H}_5)_2\text{Co}_2(\mu\text{-NO})_2$ , was first reported by Brunner in 1968.<sup>7</sup> Both the solid-state and solution-state IR spectra of this complex exhibited two  $\nu_{\text{NO}}$  indicative of a bent geometry. However, the reported crystal structure of this complex<sup>5</sup> reveals a planar geometry in contradiction to the IR spectral results. Although it is not unreasonable to assume that this complex could adopt two different solid-state structures, which these observations would seem to suggest, there have not been any reported infrared spectra of  $(\eta^5\text{-C}_5\text{H}_5)_2\text{Co}_2(\mu\text{-NO})_2$  containing only one  $\nu_{\text{NO}}$  stretch.

The  $(\eta^5\text{-C}_5\text{H}_5)_2\text{Co}_2(\mu\text{-NO})_2$  complex contains a formal Co-Co single bond and has the same electron count on the metals as octacarbonyldicobalt, which is structurally  $((\text{CO})_3\text{Co})_2(\mu\text{-CO})_2$ . Since the fragments  $(\eta^5\text{-C}_5\text{H}_5)\text{Co}$  and  $(\text{CO})_3\text{Co}$  are isolobal<sup>8</sup> and have identical electron counts, the two complexes are isolobal; therefore, it might be expected that the two complexes would exhibit similar geometric and electronic properties. However, these complexes appear to be quite different from one another. Although both complexes contain a formal Co-Co single bond, the Co-Co separations in the complexes are quite different with a Co-Co separation of 2.528 Å in  $\text{Co}_2(\text{CO})_8$ <sup>9</sup> compared to 2.372 Å in  $(\eta^5\text{-C}_5\text{H}_5)_2\text{Co}_2(\mu\text{-NO})_2$ .<sup>5</sup> In addition, octacarbonyldicobalt assumes a bent geometry whereas the solid-state structure of  $(\eta^5\text{-C}_5\text{H}_5)_2\text{Co}_2(\mu\text{-NO})_2$  appears to be planar. Pinhas and Hoffmann<sup>10</sup> studied the possible geometries of these two complexes via extended Hückel complexes and found that the puckered geometry of  $\text{Co}_2(\text{CO})_8$  was due to a tilting of the  $\text{Co}(\text{CO})_3$  groups, which imparts a directional asymmetry to the metal frontier orbitals which interact with the bridging carbonyls which, in turn, causes the complex to bend. When the cyclopentadienyl ligands were kept stationary, in a perpendicular position to a planar  $\text{Co}_2(\mu\text{-NO})_2$  core, the planar geometry of  $(\eta^5\text{-C}_5\text{H}_5)_2\text{Co}_2(\mu\text{-NO})_2$  was found to be most stable. However, when the cyclopentadienyl ligands were tilted off the perpendicular position, a bent geometry for  $(\eta^5\text{-C}_5\text{H}_5)_2\text{Co}_2(\mu\text{-NO})_2$  was found to be more stable than the planar geometry.

Not only is the geometric structure of  $(\eta^5\text{-C}_5\text{H}_5)_2\text{Co}_2(\mu\text{-NO})_2$  a source of some controversy, but the ground-state electronic structure has also been a topic of some discussion. Initially, an NMR study suggested that  $(\eta^5\text{-C}_5\text{H}_5)_2\text{Co}_2(\mu\text{-NO})_2$  possesses a singlet diamagnetic ground state.<sup>7</sup> Later, ab initio molecular

**Table I.** Bond Distances (Å) and Angles (deg) for the Various Geometries of Compounds 1 and 2

Distances					
A-B	dist	A-B	dist	A-B	dist
Co-Co	2.370	N-O	1.187	Co- $\Omega$	1.724
Co-N	1.826	C-C	1.417	Co-O	1.85
Co-C	2.101	C-H	1.05	O-H	1.00
Values of $\theta$ and $\phi$					
compd	geometry	$\theta$	$\phi$		
1	a	180.0	90.0		
2	a	179.95	90.0		
1 and 2	b	160.0	92.8		
1 and 2	c	140.0	95.6		
1 and 2	d	120.0	98.4		
1 and 2	e	100.0	101.2		

orbital calculations suggested that this complex may actually have a triplet electronic ground state.<sup>11</sup> In response to this study, magnetic susceptibility measurements were performed on this complex which concluded that it definitely had a singlet diamagnetic ground state.<sup>12</sup>

In this paper, the geometric and electronic structure of  $(\eta^5\text{-C}_5\text{H}_5)_2\text{Co}_2(\mu\text{-NO})_2$  will be examined via ab initio molecular orbital calculations. More specifically, the question of bent versus planar geometries and singlet versus triplet electronic ground states will be examined for this compound. The effects of electron correlation on  $(\eta^5\text{-C}_5\text{H}_5)_2\text{Co}_2(\mu\text{-NO})_2$  will be examined via generalized valence bond (GVB) calculations and complete active space self-consistent field (CASSCF) calculations. In order to better investigate the effects of electron correlation on the  $\text{Co}_2(\mu\text{-NO})_2$  core, some of the calculations will be performed on a model compound for  $(\eta^5\text{-C}_5\text{H}_5)_2\text{Co}_2(\mu\text{-NO})_2$ , in which the cyclopentadienyl ligands are modeled by a linear hydroxide ligand. The differences in the orbital interactions as the complex bends will be examined as well as the relationship of the electron density and chemical bonding through deformation density studies and topological analyses.

## Theoretical Methods

Ab initio molecular orbital calculations were performed on  $(\eta^5\text{-C}_5\text{H}_5)_2\text{Co}_2(\mu\text{-NO})_2$ , **1**, and its model compound  $(\text{HO})_2\text{Co}_2(\mu\text{-NO})_2$ , **2**, in various geometries which represent the molecules as they pucker. For the planar form of **1**, the experimentally determined bond lengths and angles were used after idealizing to  $C_{2v}$  symmetry (with eclipsed cyclopentadienyl rings). The  $C_{2v}$  geometry of **1** was used in these calculations because there is no change in symmetry of the molecule as it bends, unlike the  $C_{2h}$  geometry of the planar form of **1** (with staggered Cp rings) which reduces to  $C_s$  symmetry when the molecule bends. For compound **2**, the OH group was placed at a Co-O bond length of 1.85 Å at the place where the center of the cyclopentadienyl ring ( $\Omega$ ) was in compound **1**. Unfortunately, the planar geometry of **2** possesses higher symmetry ( $D_{2h}$ ) than the bent forms ( $C_{2v}$ ) so a slightly bent geometry (dihedral angle of 179.95°) was assumed to represent the planar geometry of **2**, to avoid the symmetry breaking problem.

In order to correctly simulate the puckering of compounds **1** and **2**, two angles are defined as shown in Figure 1, first, the dihedral angle,  $\theta$ , between the two  $\text{Co}_2\text{N}$  planes and second, the tilt angle,  $\phi$ , between the line from the Co atom to the center of the Cp ring for **1**, or the Co-O bond for **2**, and the line from the Co atom pointing in the  $z$  direction parallel to the  $C_2$  axis. For the planar geometry of **1**, the values of  $\theta$  and  $\phi$  are 180 and 90°, respectively. For the "planar" geometry of **2**, the values of  $\theta$  and  $\phi$  are 179.95 and 90°, respectively. To simulate the bending, as the dihedral angle  $\theta$  is decreased from 180 to 100°, the tilt angle  $\phi$  is simultaneously increased from 90 to 101.2°. All bond lengths were kept constant during the geometry changes. Calculations were performed on four bent geometries for both **1** and **2**. Values of  $\theta$  and  $\phi$  for each geometry is listed in Table I.

(7) Brunner, H. J. *Organomet. Chem.* **1968**, *12*, 517.  
 (8) Hoffmann, R. *Angew. Chem., Int. Ed. Engl.* **1982**, *21*, 71.  
 (9) Leung, P. C.; Coppens, P. *Acta Crystallogr.* **1983**, *B39*, 535; Summer, G. G.; Klug, H. P.; Alexander, L. E. *Acta Crystallogr.* **1964**, *17*, 732.  
 (10) Pinhas, A. R.; Hoffmann, R. *Inorg. Chem.* **1979**, *18*, 1979.

(11) Demuynck, J.; Mougenot, P.; Bernard, M. *J. Am. Chem. Soc.* **1987**, *109*, 2265.  
 (12) Berg, D. J.; Anderson, R. A. *J. Am. Chem. Soc.* **1988**, *110*, 4849.

The molecular orbitals were generated by using, as basis functions, the split-valence basis of Williamson and Hall<sup>13</sup> for Co. In the Huzinaga notation, this is a (432-421-31) basis set. For the bridging NO, Huzinaga's split valence (321-21) basis<sup>14</sup> was used for both N and O atoms. For the terminal ligands, either the Cp or OH ligands, a minimal (33-3) basis<sup>19</sup> was used for the C or O atoms and a (3) basis<sup>19</sup> for the H atoms. Molecular orbitals were initially generated SCF by the closed-shell Hartree-Fock Roothaan procedure.<sup>15</sup> These restricted Hartree-Fock (RHF) orbitals were used as the starting point for further calculations.

Calculations on the triplet wave function were performed via the open-shell RHF method.<sup>16</sup> The energy of this triplet wave function was compared to a one-pair generalized valence bond (GVB)<sup>17</sup> wave function in which the optimization of the GVB pair began with the singly-occupied orbitals of the triplet wave function. Additionally, the effects of correlation on the  $\text{Co}_2(\mu\text{-NO})_2$  ring were studied on the model compound **2** via a five-pair GVB wave function in which the five pairs represent the bonding and antibonding combinations of the four Co-N bonds and the Co-Co "out-of-plane"  $\pi$  bond.

The electron density of compounds **1** and **2** and its relationship to chemical bonding shall be studied via two methods, a fragment deformation density study and a topological analysis of the charge density. A deformation density is defined as the difference of the molecular density and the density of an arbitrary reference called a promolecule. The promolecule ideally represents the various parts of the molecule before bonding takes place; thus, the difference in density should represent the changes in density which occur upon chemical bonding. For the fragment deformation density maps employed in this study, the promolecule consisted of two triplet CpCo fragments (or HCo fragments in the case of compound **2**) with one electron in each Co  $d_x$  orbital and two NO molecules with one electron occupying the  $2\pi$  orbital parallel to the Co-Co axis ( $2\pi^-$ ). All of the constituent parts of the promolecule are in the same geometry as the parent molecule.

The topology of the charge density was studied in order to determine whether the charge is locally concentrated or depleted in the internuclear regions.<sup>18,19</sup> This analysis utilizes both the gradient ( $\nabla\rho$ ) and the Laplacian ( $\nabla^2\rho$ ) of the charge density. Points at which the gradient is zero are called critical points. Critical points are denoted by their rank, the number of nonzero eigenvalues they possess, and their signature, the sum of the signs of the eigenvalues. In three dimensional space, there are four types of stable critical points: (3,+3) cage critical points, (3,+1) ring critical points, (3,-1) bond critical points, and (3,-3) critical points, which generally occur at atomic nuclei. A necessary requirement for the existence of a bond between two atoms is that there be an atomic interaction line called a bond path on which the density is a maximum in all directions perpendicular to the atom-atom axis. At the point where the bond path crosses the zero-flux line between the two atoms there is a (3,-1) critical point.

All maps generated from the deformation density study and the topological analysis as well as any molecular orbital plots were generated using an interactive version of MOPLLOT.<sup>20</sup> Density plots are contoured geometrically with each contour differing by a factor of 2. The absolute value of the smallest contour level has a value of  $3.90265 \times 10^{-3} e$  (au)<sup>-3</sup>. All molecular orbital calculations were performed using the GAMESS<sup>21</sup> package of programs.

- (13) Williamson, R. L.; Hall, M. B. *Int. J. Quantum Chem. Quantum Chem. Symp.* **1987**, *21*, 503.
- (14) Huzinaga, S., Ed. *Gaussian Basis Sets for Molecular Orbital Calculations*; Elsevier: Amsterdam, 1984.
- (15) Roothaan, C. C. *J. Rev. Mod. Phys.* **1951**, *23*, 69.
- (16) Roothaan, C. C. *J. Rev. Mod. Phys.* **1960**, *32*, 179.
- (17) Bobrowicz, F. W.; Goddard, W. A. In *Methods of Electron Structure Theory*; Schaefer, H. F., Ed.; Plenum: New York, 1977.
- (18) (a) Bader, R. F. W.; Nguyen-Deng, T. T.; Tal, Y. *Rep. Prog. Phys.* **1981**, *44*, 893. (b) Bader, R. F. W.; Essen, H. *J. Chem. Phys.* **1984**, *80*, 1943.
- (19) Bader, R. F. W.; MacDougall, P. J.; Lau, C. D. H. *J. Am. Chem. Soc.* **1984**, *106*, 1594.
- (20) Interactive MOPLLOT: A package for the interactive display and analysis of molecular wave functions incorporating the program MOPLLOT (D. Lichtenburger), PLOTDEN (R. F. W. Bader, D. J. Kenworthy, P. M. Beddal, G. R. Runtz, and S. G. Anderson), SCHUSS (R. F. W. Bader, G. R. Runtz, S. G. Anderson, and F. W. Biegler-Koenig), and EXTREM (R. F. W. Bader and F. W. Biegler-Koenig), P. Sherwood and P. J. MacDougall, 1989.
- (21) M. F. Guest, Daresbury Laboratories, Daresbury, U.K., provided GAMESS (Generalized Atomic and Molecular Electronic Structure System) version 4.0, 1989).

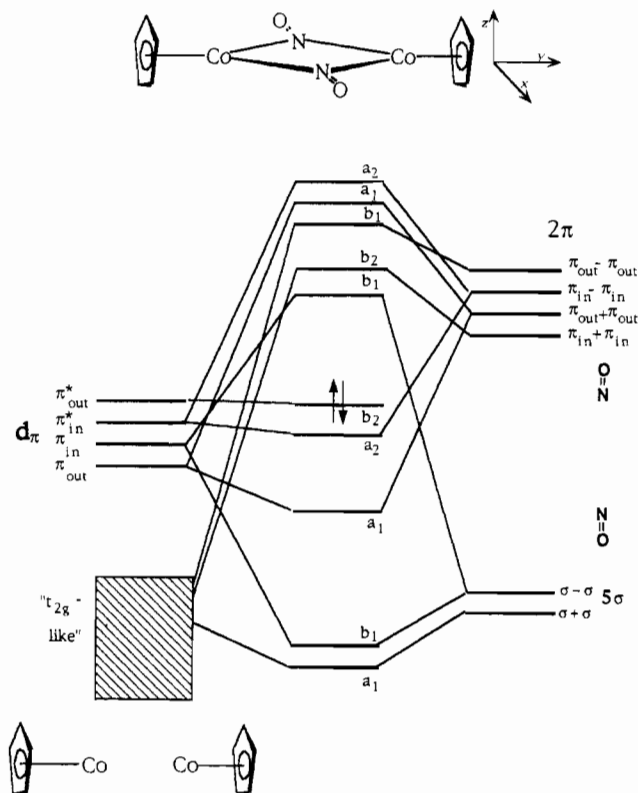


Figure 2. Qualitative molecular orbital interaction diagram between the metal  $d$  orbitals of two CpCo fragments and two bridging nitrosyl ligands.

## Results and Discussion

A qualitative molecular orbital diagram which shows the interactions between the metal  $d$  orbitals and the bridging ligand orbitals necessary to form the  $\text{Co}_2\text{N}_2$  framework is shown in Figure 2. This interaction diagram is similar to those presented in earlier theoretical studies<sup>11,22</sup> and will be briefly reviewed in order to more clearly understand the controversy in the assignment of the ground-state electronic structure of **1**. This diagram shows the interaction between the cobalt atoms  $d_x$  and  $d_y$  orbitals and the nitrosyls'  $5\sigma$  and  $2\pi$  orbitals. The overall symmetry of the molecule is assumed to be  $C_{2v}$ , and the coordinate system employed in the diagram is the same as the one which was assigned by the GAMESS program which places the  $z$  axis on the principal rotation axis ( $C_2$ ), the  $y$  axis parallel to the Co-Co axis, and the  $x$  axis parallel to the ON...NO axis.

In the  $(\eta^5\text{-C}_5\text{H}_5)\text{Co}$  fragment, the cyclopentadienyl ligand, hereafter referred to as the Cp ligand, splits the cobalt  $d$  orbitals into the familiar octahedral splitting of 2 over 3 orbitals. The "t<sub>g</sub>-like" orbitals consist of the  $d_{y^2}$ ,  $d_{x^2-y^2}$ , and  $d_{xz}$  orbitals and the "e<sub>g</sub>-like" orbitals consist of the  $d_{xy}$  and  $d_{yz}$  orbitals. The interaction of two CpCo fragments with each other will create combinations of these orbitals which can be related to Co-Co  $\sigma$ ,  $\pi$ , and  $\delta$  bonding and antibonding orbitals. The combinations deriving from the "t<sub>g</sub>-like" orbitals form the Co-Co  $\sigma$ ,  $\sigma^*$ ,  $\delta$ , and  $\delta^*$  orbitals and those from the "e<sub>g</sub>-like" orbitals form the Co-Co  $\pi$  and  $\pi^*$  orbitals. The Co-Co  $\pi$  and  $\pi^*$  orbitals can be further differentiated with respect to the  $\text{Co}_2(\mu\text{-NO})_2$  plane as residing either in the plane (sometimes referred to as parallel) or out of the plane (sometimes referred to as perpendicular). So, the Co-Co  $\pi$ -type orbitals can be notated as  $\pi_{in}$  and  $\pi_{out}$  orbitals or  $\pi_{in}^*$  and  $\pi_{out}^*$  orbitals. These orbitals interact mainly with the bridging nitrosyls'  $5\sigma$  and  $2\pi$  orbital combinations. The nitrosyls'  $2\pi$  orbital combinations will also be classified as lying in or out of the  $\text{Co}_2\text{N}_2$  plane.

The major interactions between the fragment orbitals which occur upon formation of **1** involve the Co-Co  $\pi$ -type orbitals and the nitrosyls'  $5\sigma$  and  $2\pi$  orbitals. The Co-Co  $\pi_{in}$  orbital interacts

- (22) Schugart, K. A.; Fenske, R. F. *J. Am. Chem. Soc.* **1986**, *108*, 5094.

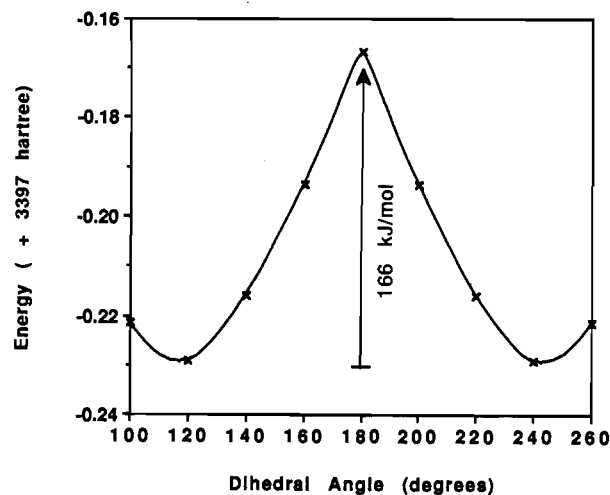
**Table II.** Wave Function Energies for Various Geometries of Compounds 1 and 2

Compound 1 (+3397 hartree)				
dihedral angle (deg)	RHF	triplet	GVB	
100	-0.221 506	-0.326 761	-0.341 033	
120	-0.229 850	-0.339 149	-0.351 206	
140	-0.215 850	-0.334 127	-0.342 379	
160	-0.193 507	-0.322 038	-0.327 670	
180	-0.166 573	-0.312 741	-0.313 572	
Compound 2 (+3165 hartree)				
dihedral angle (deg)	RHF	triplet	GVB-1	GVB-5
100	-0.348 165	-0.487 533	-0.496 686	-0.547 786
120	-0.357 984	-0.501 673	-0.507 926	-0.557 678
140	-0.348 416	-0.499 163	-0.501 856	-0.550 915
160	-0.330 442	-0.493 040	-0.493 756	-0.542 422
179.95	-0.308 517	-0.490 398	-0.490 787	-0.539 276

strongly with the out-of phase, "minus" combination of the nitrosyls'  $5\sigma$  orbitals, thereby raising the energy of the  $\pi_{in}$  orbital. The Co-Co  $\pi_{out}$  orbital interacts with the higher-lying nitrosyl  $2\pi_{out}$  "plus" combination, thereby lowering its energy. The Co-Co  $\pi_{in}^*$  orbital interacts with the nitrosyl  $2\pi_{in}$  "minus" combination, which lowers its energy. The Co-Co  $\pi_{out}^*$  orbital is not able to interact with any nitrosyl orbital even though, in  $C_{2v}$  symmetry, there is a nitrosyl  $2\pi$  combination of the appropriate symmetry. The reason that they do not interact is that the metal-based orbital points toward the nodes of the ligand-based orbital so the two orbitals are not able to overlap enough to interact significantly. The remainder of the interactions between the nitrosyl and the cobalt d orbitals are weaker and involve the "t<sub>2g</sub>-like" cobalt d orbitals. The "plus" combination of nitrosyl  $5\sigma$  orbitals lowers its energy through interaction with the Co-Co  $\sigma$  orbital and with a high lying  $4s$  or  $sp$  hybrid (not shown on Figure 2). The remaining nitrosyl  $2\pi$  orbitals which do not interact with the cobalt's  $\pi$ -type orbitals (the "plus" combination of the  $2\pi_{in}$  and the "minus" combination of the  $2\pi_{out}$  orbitals) raise their energy through interaction with some of the "t<sub>2g</sub>-like" orbitals.

Upon filling of this molecular orbital diagram with the appropriate number of electrons, the HOMO turns out to be the Co-Co  $\pi_{out}^*$  orbital ( $b_2$ ). Of the four Co-Co  $\pi$ -type orbitals, only the Co-Co  $\pi_{in}$  ( $b_1$ ) is unoccupied. Note that the two Co-Co  $\pi$ -antibonding orbitals are filled, whereas only one of the Co-Co  $\pi$ -bonding orbitals is filled. This description of the electronic structure of compound 1 is similar to the result obtained from extended Hückel,<sup>10</sup> Fenske-Hall,<sup>22</sup> and DV- $X\alpha$ <sup>23</sup> calculations. However, later ab initio molecular orbital calculations<sup>11</sup> performed on 1 found that when the orbital consisting mostly of the nitrosyl  $2\pi_{out}$  "plus" combination ( $a_1$ ) is occupied instead of the Co-Co  $\pi_{out}^*$  orbital, ( $b_2$ ) the resulting electron configuration was lower in energy than the configuration previously described. This lower energy singlet electron configuration was obtained later in another ab initio molecular orbital calculation.<sup>24</sup> In addition, it was found that the energy of an open-shell triplet wave function which singly occupied both the Co-Co  $\pi_{out}^*$  ( $b_2$ ) and nitrosyl  $2\pi_{out}$  plus combinations ( $a_1$ ) was lower in energy by 1.3 mhartrees (3 kJ) than the energy of a two-configuration MCSCF wave function which contained both of these singlet electron configurations. This led the authors to propose that the electronic ground state of 1 could be a triplet electronic state.<sup>11</sup>

**Ground-State Geometry of  $(\eta^5\text{-C}_5\text{H}_5)_2\text{Co}(\mu\text{-NO})_2$ .** A list of wave function energies for the different geometries on which calculations have been performed for both compounds 1 and 2 is shown in Table II. Graphs of wave function energy versus dihedral angle for compounds 1 and 2 were calculated for the

**Figure 3.** Plot of the RHF wave function energy versus  $\text{Co}_2(\mu\text{-N})\text{-Co}_2(\mu\text{-N}')$  dihedral angle for  $(\text{C}_5\text{H}_5)_2\text{Co}_2(\mu\text{-NO})_2$ .

various different electronic configurations. For the graphs, the plots include points on the other "side" of the planar geometry ( $\phi = 180^\circ$ ) which are symmetrically equivalent (or nearly equivalent) to the calculated points. A line was interpolated between the points to qualitatively simulate the potential surface of the molecule. All of these graphs were quite similar.

A typical graph of the RHF wave function energy versus dihedral angle for compound 1 is shown in Figure 3; for both compounds, the planar geometry has the highest energy and the lowest energy geometry possesses a dihedral angle of  $120^\circ$ . The energy difference between these two geometries is 63.3 mhartree (170 kJ/mol) for compound 1 and 49.5 mhartree (130 kJ/mol) for compound 2. This quite sizeable barrier to the planar geometry would suggest that the geometry of an isolated  $(\eta^5\text{-C}_5\text{H}_5)_2\text{Co}_2(\mu\text{-NO})_2$  molecule is bent. This is in agreement with the experimental observations of a bent structure in both the vapor and solution-phases of 1 ( $\nu_{\text{NO}}$ ) but not with the observed planar solid-state structure (single-crystal X-ray diffraction). The calculated energies for the various geometries of 1 suggest a very large energy barrier to the planar geometry. It is much too large to be compensated for in the solid state by the effects of crystal packing which usually are of the order of a few kilojoules per mole.<sup>25</sup>

This discrepancy between theoretical and experimental geometries immediately leads to questions about the level of the theoretical calculation. Perhaps the addition of some electron correlation would lower the energy barrier to a planar geometry so that crystal packing effects in the crystal could compensate for it. The simplest method of adding correlation to the  $\text{Co}_2(\mu\text{-NO})_2$  core is through a one-pair GVB wave function which correlates the HOMO of the RHF wave function, which is a Co-Co  $\pi_{out}^*$  orbital of  $b_2$  symmetry, with the metal-ligand antibonding combination of the Co-Co  $\pi_{out}$  and the NO  $2\pi_{out}$  orbitals of  $a_1$  symmetry. For both 1 and 2, correlation of this pair of electrons leads to a very large drop in energy from the RHF wave function, on the order of 130 mhartree for 1 and 160 mhartree for 2, indicative of a large amount of correlation error for these electrons.

Plots of GVB wave function energy versus dihedral angle for 1 and 2 again show a maximum at  $180^\circ$  and a minimum at  $120^\circ$ . Once again, the planar geometry has the highest energy but now the energy barrier has been reduced to 37.6 mhartree (99 kJ/mol) for 1 and to 17.1 mhartree (45 kJ/mol) for 2. Although the reduction in the energy barrier for the one-pair GVB wave function is significant, this barrier still remains quite large. Perhaps if larger amounts of electron correlation are included, the energy barrier to a planar structure will be decreased enough to bring

(23) Pilloni, G.; Zecchin, S.; Casarin, M.; Granozzi, G. *Organometallics* 1987, 6, 597.(24) Quelch, G. E.; Hillier, I. H. *Chem. Phys. Lett.* 1988, 144, 153.(25) Brock, C. P. *Acta Crystallogr., Sect. A* 1977, A33, 193. Bernstein, J.; Hagler, A. T. *J. Am. Chem. Soc.* 1978, 100, 673.

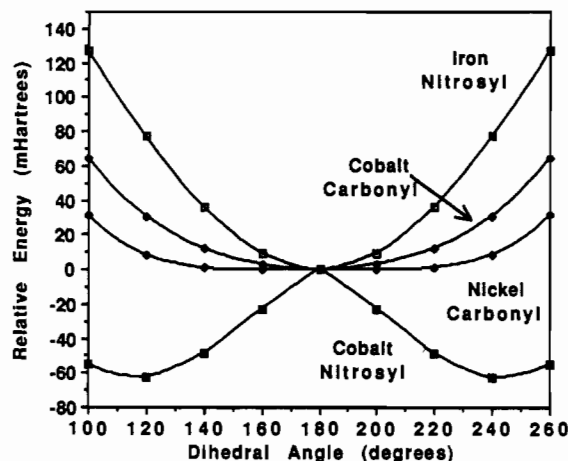


**Figure 4.** Plot of the relative RHF wave function energy versus  $M_2(\mu-A)-M_2(\mu-A')$  dihedral angle for  $Cp_2M_2(\mu-AO)_2$  complexes ( $M = Fe, A = N; M = Co, A = N$  and  $C; M = Ni, A = C$ ).

the theoretical calculations in line with the experimental observations. The large size of the ab initio molecular orbital calculations on  $(\eta^5-C_5H_5)_2Co_2(\mu-NO)_2$  makes it difficult to introduce large amounts of electron correlation into the wave function. Therefore, additional calculations were performed only on model 2. Thus far, the wave function and energies reported for both the Cp dimer and its model compound behave similarly.

A five-pair GVB calculation was performed on 2 in which the five GVB pairs represent the interactions among the electrons in the four Co-Co  $d_x$  orbitals and the six nitrosyl  $5\sigma$  and  $2\pi$  orbitals. Once again, the planar geometry is higher in energy by 18.4 mhartree (48 kJ/mol). This barrier is slightly higher than that for the one-pair GVB wave function (45 kJ/mol) and would seem to suggest that additional electron correlation would not significantly lower the energy barrier to the planar geometry.

The results of these calculations point to a more stable bent geometry for  $(\eta^5-C_5H_5)_2Co_2(\mu-NO)_2$ . The planar geometry is much higher in energy with the lowest calculated barrier at 45 kJ/mol for the model compound. This result is in dramatic contrast to the experimental observation of a planar structure in the solid state for  $(\eta^5-C_5H_5)_2Co_2(\mu-NO)_2$ .

**Comparison of Structure  $Cp_2M_2(\mu AO)_2$ .** In order to determine whether calculations at this level of theory would agree with experiments on the structure of the other complexes in this family, closed-shell RHF calculations were performed for the complexes  $(\eta^5-C_5H_5)_2Fe_2(\mu-NO)_2$ ,  $(\eta^5-C_5H_5)_2Co_2(\mu-CO)_2$ , and  $(\eta^5-C_5H_5)_2Ni_2(\mu-CO)_2$  in the same fashion as 1. Plots of RHF wave function relative energy versus dihedral angle are shown in Figure 4. The plotted energies are relative to the energy of the planar geometry for each molecule. For the iron nitrosyl complex, the planar geometry is the most stable with all of the bent geometries lying much higher in energy. This is consistent with the observed planar geometry in the solid-state geometry of  $(\eta^5-C_5H_5)_2Fe_2(\mu-NO)_2$ . Likewise, the cobalt carbonyl complex exhibits the same type of potential surface as the iron nitrosyl except that the bent geometries lie somewhat lower in energy (that is, a softer potential curve about the planar geometry). This is consistent with the experimental observation of planar geometries for most cobalt carbonyl complexes along with a slightly bent geometry (dihedral angle of  $176^\circ$ ) for  $(\eta^5-C_5Me_5)_2Co_2(\mu-CO)_2$ . The potential surface for the nickel carbonyl complex is very flat about the planar geometry. In fact, up to a dihedral angle of  $120^\circ$ , the RHF energy is within 20 kJ/mol of the planar geometry. This is consistent with the experimental observations of an bent structure for  $(\eta^5-C_5H_5)_2Ni_2(\mu-CO)_2$  and a planar structure for  $(\eta^5-C_5H_4Me)_2Ni_2(\mu-CO)_2$ . The only complex whose theoretically calculated geometry differs widely from the experimentally determined one is  $(\eta^5-C_5H_5)_2Co_2(\mu-NO)_2$ .

The theoretical calculations on  $(\eta^5-C_5H_5)_2Co_2(\mu-NO)_2$  indicate that an isolated molecule will adopt a bent geometry. It would

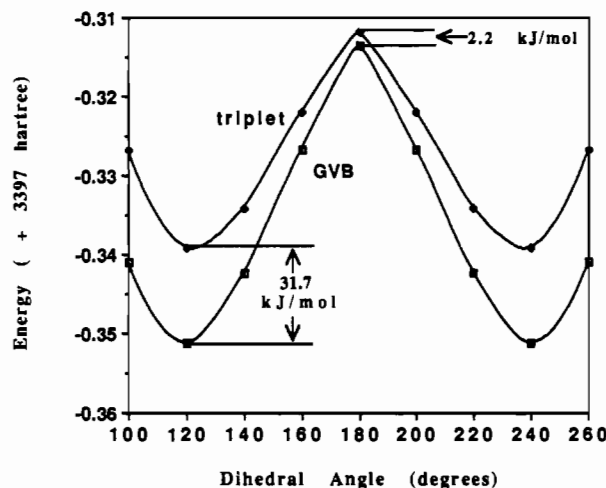


**Figure 5.** Plot of wave function energies versus dihedral angle for the open-shell RHF triplet and GVB wave functions of  $Cp_2Co_2(\mu-NO)_2$ .

seem that the planar form of this molecule is so much higher in energy that the effects of crystal packing could not possibly force this molecule to be planar, a direct contradiction with the reported crystal structure analysis. This crystal structure analysis is also contrary to the observation of two  $\nu_{NO}$  stretches in the solid-state IR spectrum of 1.<sup>7</sup> This is the only reported case in this group of dinuclear complexes in which the reported solid-state IR spectrum disagrees with the solid-state structure obtained by X-ray diffraction.

**Singlet vs Triplet Electronic States.** As shown in the plot in Figure 5, our two configurations GVB wave function (GVB-1 pair) has a lower energy than the corresponding triplet wave function for every geometry of 1. The energy difference between the two wave functions is smallest for the planar geometry with an energy difference of 0.83 mhartree (or 2.2 kJ/mol) between the triplet and GVB wave function. This difference gets larger as the molecule bends with a difference of 12.06 mhartree (31.7 kJ/mol) for the  $120^\circ$  geometry. The lower energy of the GVB wave function leads to the conclusion that  $(\eta^5-C_5H_5)_2Co_2(\mu-NO)_2$  has a diamagnetic electronic ground state in agreement with the experimental magnetic susceptibility measurements.<sup>12</sup>

Even though this result does not agree with those obtained by Benard et al.,<sup>11</sup> it is not drastically different. The authors of that study found that for the planar molecule (they did not investigate bent geometries), the triplet state was lower in energy by 1.3 mhartree (3.4 kJ/mol) from the two-configuration singlet state. When compared to the present calculations, this is only a difference 2.1 mhartree (or 5.5 kJ/mol), which is well within the limits of uncertainty for these calculations. This difference most likely originates from the choice of atomic basis set.

The small energy difference between the triplet and singlet electronic states for the planar geometry of 1 would suggest that if the molecule was indeed planar, some evidence of a low-lying triplet electronic state should be observed at higher temperatures. The lack of any such evidence leads to the conclusion that the molecule is bent in the solid state because there the energy of the triplet state is much higher than that of the singlet state.

**Effects of Electron Correlation on the  $Co_2N_2$  Core.** The GVB calculations for both compounds 1 and 2 exhibit the same general features with respect to the bending of the  $Co_2N_2$  core. The GVB pair consists of the HOMO from the RHF wave function, which is a Co-Co  $\pi^*_{out}$  orbital of  $b_2$  symmetry, and the LUMO, which is a cobalt-nitrosyl antibonding combination of the Co-Co  $\pi_{out}$  orbital and the nitrosyl  $2\pi_{out}$  orbitals of  $a_1$  symmetry. These two orbitals interact very strongly in the GVB wave function as shown by the drop in energy when the GVB wave function. The correlation energy (i.e., GVB energy minus RHF energy) of this one-pair GVB wave function ranges from 182.3 mhartree for the planar geometry to 148.5 mhartree for the  $100^\circ$  geometry. This is quite a sizeable drop in energy for a single pair GVB.

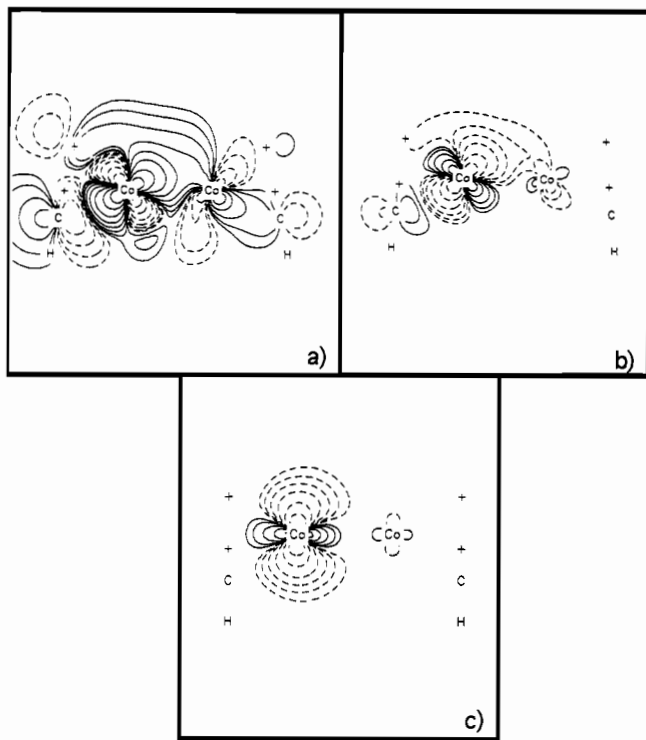


**Figure 6.** Molecular orbital plot of one of the GVB pair orbitals for the 100° (a), 140° (b), and 180° (c) geometries of  $\text{Cp}_2\text{Co}_2(\mu\text{-NO})_2$ . Plots are shown in the plane containing both metal atoms and one of the carbon and hydrogen atoms of the cyclopentadienyl ligand. This plane corresponds to the plane perpendicular to the  $\text{Co}_2(\mu\text{-NO})_2$  plane in the planar geometry. Plots are contoured geometrically with each contour level differing by a factor of 2. The absolute value of the smallest contour level has a value of  $3.90265 \times 10^{-3} \text{ e (au)}^{-3}$ .

A GVB pair can be expressed in molecular orbitals terms by plotting GVB natural orbitals which correspond to delocalized bonding and antibonding combinations of the GVB pair orbitals, or they can be plotted as localized GVB pair orbitals. Plots of the GVB pair orbitals from the one pair GVB calculations of 1 are shown for the 100, 140, and 180° geometries in Figure 6. They are plotted in the plane which is perpendicular to the original planar  $\text{Co}_2\text{N}_2$  core (the  $yz$  plane). As one progresses from bent to planar geometries, interesting changes occur in these GVB pair orbitals. The 100° GVB pair orbital, shown in Figure 6a, consists mostly of a Co  $d_{yz}$  orbital ( $\pi_{\text{out}}$ ) on one of the cobalt atoms. In addition, there is a significant amount of  $d_{yz}$  character on the other cobalt, which is bonding with respect to the first Co atom. This observation is indicative of some degree of covalent bonding between the two cobalt atoms. The companion to this GVB pair orbital is the mirror image with the major amount of d orbital character on the other cobalt atom. When these two pair orbitals combine to form the natural orbitals, the resulting orbitals are reminiscent of the bent Co–Co bonding and antibonding orbitals which are found for octacarbonyl dicobalt.<sup>26</sup>

The 140° GVB pair orbital, shown in Figure 6b, is fairly similar to the 100° GVB pair orbital. The main difference between the two is that the relative amounts of d orbital character on each cobalt atom have changed with more of the orbital character residing on one of the cobalts at the expense of the other cobalt. This is indicative of a lesser degree of covalent bonding between the cobalts than in the 100° geometry. As in the 100° geometry, the 140° pair orbitals combine to form natural orbitals which are reminiscent of bent Co–Co bonding and antibonding orbitals.

The 180° GVB pair orbital, shown in Figure 6c, is significantly different from the GVB pair orbitals at the previous bent geometries. All of the cobalt  $d_x$  orbital character has been removed and replaced by a nonbonding  $d_{x^2-y^2}$  orbital on one of the

**Table III.** Natural Orbital Occupancies for GVB Calculations on Compounds 1 and 2

	100°	120°	140°	160°	180°
Compound 1, One-Pair GVB					
$a_1$	1.393 374	1.355 284	1.301 589	1.224 967	1.102 710
$b_2$	0.606 226	0.644 716	0.698 412	0.775 033	0.897 290
Compound 2, One-Pair GBV					
$a_1$	1.324 753	1.282 511	1.191 055	1.081 177	1.053 268
$b_2$	0.675 247	0.717 489	0.809 845	0.918 823	0.946 732
Compound 2, Five-Pair GVB					
Co–Co	1.317 689	1.273 136	1.178 080	1.076 738	1.049 951
	0.682 312	0.726 264	0.821 920	0.923 262	0.950 049
Co–N(av)	1.987 043	1.987 483	1.987 828	1.988 071	1.988 170
	0.012 957	0.012 517	0.012 172	0.011 929	0.011 830

cobalt atoms. There is a very small amount of  $d_x$  character on the other cobalt atom, but there is no orbital overlap between the two cobalt atoms, indicative of no direct interaction between the cobalt atoms. The other GVB pair orbital is the mirror image of the first orbital with the major portion of it residing on the other cobalt atom. When these pair orbitals combine to form natural orbitals, the resultant orbitals form essentially Co–Co nonbonding orbitals which consist mainly of in and out-of-phase combinations of Co  $d_x$  orbitals with little direct Co–Co interaction.

Table III lists the natural orbital occupancies for the one pair GVB calculations on 1, as well as those for the one- and five-pair GVB calculations on 2. If we look at the natural orbital occupancies for the 100° geometry of 1, note that the  $a_1$  bonding natural orbital has an occupancy of 1.393 e compared to 0.606 e for the  $b_2$  antibonding natural orbital. As the dihedral angle increases, the occupancy of the  $a_1$  natural orbital decreases and that of the  $b_2$  orbital increases. For the planar geometry, the natural orbital occupancies of the  $a_1$ ,  $b_2$  pair are almost equal at 1.103 and 0.897 e, respectively. Single occupancy of two nonbonding GVB natural orbitals indicates that the planar molecule is described best as a singlet radical pair with no direct Co–Co interaction.

The five-pair GVB wave function was derived from localized orbitals of compound 2. In an earlier study on  $\text{Co}_2(\text{CO})_8$ ,<sup>26</sup> a localization of the canonical molecular orbitals with the Boys criterion<sup>27</sup> resulted in localized orbitals corresponding to separate Co–Co and Co–C<sub>br</sub> bonding orbitals. When a similar localization is performed on both 1 and 2, the resulting orbitals also correspond to separate Co–Co and Co–N bonding orbitals. The five-pair GVB pairs were generated in compound 2 from the five localized Co–N and Co–Co bonding orbitals. The five-pair GVB wave function should include the “near degenerate” correlation inherent in the Co–Co and the four Co–N bonds.

If the energies of the one-pair and the five-pair GVB wave functions for 2 are compared, the drop in energy due to the addition of the four extra GVB pairs is much smaller than the correlation energy obtained from the one-pair GVB calculation. For example, for the planar geometry of 2, the energy of the five-pair GVB wave function is 48.5 mhartree lower than that of the one-pair GVB wave function, but the one-pair GVB wave function is, in turn, 182.3 mhartree lower than that of the RHF energy. Therefore, the correlation of the near degenerate Co–Co election pair contributes roughly 79% of the total correlation energy in the five-pair GVB wave function. The contribution of the Co–Co pair to the five-pair GVB wave function correlation energy shrinks slightly as the molecule bends, to 76% for the 140° geometry and to 74% for 100° geometry. Basically, the main conclusion is that a major portion of the “near-degenerate” correlation energy in the  $\text{Co}_2\text{N}_2$  “ring” derives from the Co–Co interaction.

The main conclusion that can be derived from the GVB calculations suggests the existence some degree of direct Co–Co covalent bonding in the bent geometries of  $(\eta^5\text{-C}_5\text{H}_5)_2\text{Co}_2(\mu\text{-NO})_2$ .

(26) Low, A. A.; Kunze, K. L.; MacDougall, P. J.; Hall, M. B. *Inorg. Chem.* **1991**, *30*, 1079.

(27) Foster, J. M.; Boys, S. F. *Rev. Mod. Phys.* **1960**, *32*, 300.

NO)<sub>2</sub>. The amount of direct bonding between the cobalt atoms decreases as the molecule approaches planarity. When the molecule adopts a planar geometry, no direct Co–Co interaction exists and pair of electrons involved in the direct interaction evolve into a singlet radical pair of electrons occupying the perpendicular  $d_{yz}$  on each cobalt atom. This observation of a direct interaction between the cobalts in the bent geometry evolving into no direct interaction in the planar geometry has been suggested previously by discrete variational calculations on  $(\eta^5\text{-C}_5\text{H}_5)_2\text{Co}_2(\mu\text{-NO})_2$ .<sup>23</sup>

**Density Analysis. Deformation Density Study.** Deformation density studies have been commonly employed to study the relationship of electron density to chemical bonding in many transition metal complexes.<sup>28</sup> A common observation for practically all deformation density studies is that the “standard” deformation density which uses the collection of spherically averaged atoms as the promolecule does not isolate sufficiently the density changes due to metal–metal bonding<sup>29</sup> from the density changes due to the crystal field or ligand bonding. Some thought must be put into the appropriate choice of promolecule before deformation density maps can be obtained which exhibit accumulations, if any, which can be associated with metal–metal bonding.

For a deformation density study of  $(\eta^5\text{-C}_5\text{H}_5)_2\text{Co}_2(\mu\text{-NO})_2$ , a plausible choice for a promolecule might be the density of two  $(\eta^5\text{-C}_5\text{H}_5)\text{Co}$  fragments with one electron in each  $d_{yz}$  orbital as well as the density of two neutral nitrosyl molecules with one electron in the  $2\pi_{in}$  orbital. The densities of the fragments were recalculated for each different geometry of  $(\eta^5\text{-C}_5\text{H}_5)_2\text{Co}_2(\mu\text{-NO})_2$  so that the fragments had the same location and orientation as the original molecule. The resultant deformation density maps are plotted: in the  $yz$  plane, which contains the cobalt atoms, the 2-fold axis of the molecule, and one of the CH groups of the Cp ligand; in the plane which contains both cobalt atoms and one of the nitrosyl ligands; in the  $xz$  plane, which contains both nitrosyl ligands and is perpendicular to the Co–Co axis. The deformation density maps were calculated for both the RHF and GVB wave functions of  $(\eta^5\text{-C}_5\text{H}_5)_2\text{Co}_2(\mu\text{-NO})_2$ .

The deformation density maps for the 180° geometry in the  $yz$  plane (containing the cobalt atoms and perpendicular to the  $\text{Co}_2\text{N}_2$  plane) are shown for the RHF wave function in Figure 7a and for the GVB wave function in Figure 7d. Both maps possess large accumulation regions about the cobalt atoms in the region of the out-of-plane  $d_{yz}$  orbital. All accumulation regions between the two cobalt atoms in this plane appear to be associated with extra accumulation in the cobalt  $d$  orbital and cannot be attributed to direct metal–metal bonding. The accumulation in the cobalt  $d$  orbital in the RHF map seems to be skewed away from the in-plane carbon atom. This skewing of the accumulation region virtually disappears in the GVB map. There is also a deficit region about the cobalt atom perpendicular to the Co–Co axis. This perpendicular deficit grows larger in the GVB maps presumably due to a smaller occupation in the perpendicular  $d_{yz}$  orbital.

These observations are consistent with the analysis of the GVB wave functions in the previous section. As shown in the GVB pair orbitals for the 180° geometry, the GVB wave function suggested two nonbonding singly occupied  $d_{yz}$  orbitals instead of an out-of-plane Co–Co bent bond. In order for this to occur, the  $d_{yz}$  orbitals which were doubly occupied in our simple molecular orbital picture of compound 1 must become singly occupied with the “extra” electrons moving to the out-of-plane  $d_{yz}$  orbital. In the promolecule, the  $d_{yz}$  orbital is doubly occupied and the  $d_{yz}$  orbital is singly occupied. Therefore, when the promolecule

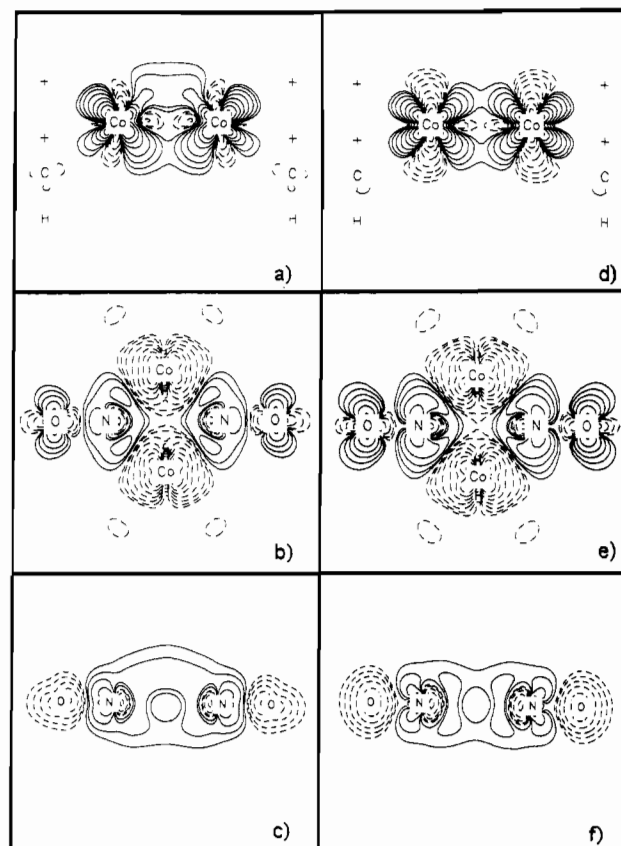


**Figure 7.** Deformation density maps of  $\text{Cp}_2\text{Co}_2(\mu\text{-NO})_2$  in the planar geometry for the RHF wave function in (a) the  $yz$  plane perpendicular to the  $\text{Co}_2(\mu\text{-NO})_2$  plane; (b) the  $xy$  plane containing the  $\text{Co}_2(\mu\text{-NO})_2$  plane, and (c) the  $xz$  plane containing the nitrosyl ligands and for the five-pair GVB wave function in (d) the  $yz$  plane, (e) the  $xy$  plane, and (f) the  $xz$  plane. Contouring is as in Figure 6.

density is subtracted from the molecular density, the resultant deformation density maps exhibit large accumulations in the  $d_{yz}$  orbital region and deficits in the  $d_{yz}$  region. None of the features present in the deformation density in this plane can be attributed to any direct bonding interaction between the two cobalt atoms. In fact, the observation of doubly occupied  $d_{yz}$  orbitals on each cobalt atom might suggest some type of antibonding interaction between the cobalt atoms.

The deformation density in the  $xy$  plane containing the cobalt atoms and the nitrosyl ligands is shown for the RHF wave function in Figure 7b and for the GVB wave function in Figure 7e. In both maps, there is substantial nitrosyl  $\pi$  accumulation even though the promolecule already contains an electron in the  $2\pi_{in}$  orbital. The  $\pi$  accumulation is larger in the GVB map. There is a separate accumulation region in the RHF maps which can be attributed to a bond between the cobalt and nitrogen atoms. In the GVB maps, the bond accumulation is an extension of the  $\pi$  accumulation region. These observations are indicative of strong Co–N bonds. Also consistent with the notion of metal to ligand  $\pi$  charge donation, there are large density deficit regions in the cobalt  $d_{yz}$  orbital in this plane with simultaneous  $\pi$  accumulations in the nitrosyl ligands. The density loss about the cobalt atom is greater in the GVB maps indicative of greater  $\pi$  donation in the GVB wave function. Additionally, ligand to metal  $\sigma$  donation can also be observed in both maps by the deficit regions in the nitrosyl's  $\sigma$  region and the accumulation region surrounding this deficit region in the area toward the center of the  $\text{Co}_2\text{N}_2$  ring.

The deformation density maps for the 180° geometry in the plane containing the two nitrosyl ligands and perpendicular to the Co–Co axis are shown for the RHF wave function in Figure 7c and for the GVB wave function in Figure 7f. Both maps exhibit the expected  $\pi$  accumulation and  $\sigma$  deficit regions about the nitrosyl ligands. These accumulation regions about the nitrosyl

(28) For a recent review see: (a) Low, A. A.; Hall, M. B. In *Theoretical Models of Chemical Bonding, Part 2: The Concept of the Chemical Bond*; Maskic, F. B., Ed.; Springer Verlag: New York, 1990. (b) Coppens, P.

(29) For a more detailed discussion see: Hall, M. B. In *Electron Distributions and the Chemical Bond*; Coppens, P., Hall, M. B., Eds.; Plenum: New York, 1982; p 205.

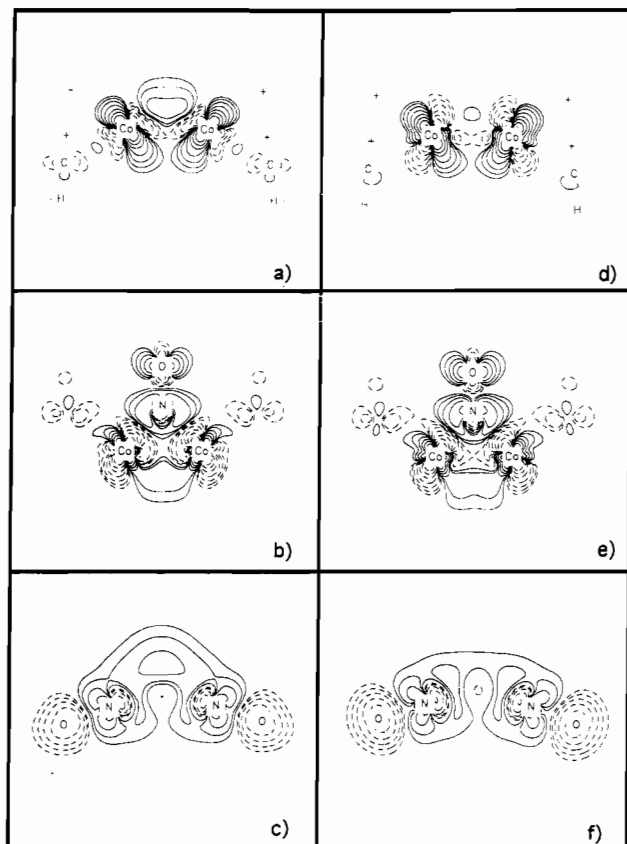


**Figure 8.** Deformation density maps for  $\text{Cp}_2\text{Co}_2(\mu\text{-NO})_2$  in the  $140^\circ$  geometry for the RHF wave function in (a) the  $yz$  plane, (b) the plane containing both cobalt atoms and one nitrosyl ligand, and (c) the  $xz$  plane and for the five-pair GVB wave function in (d) the  $yz$  plane, (e) the plane containing both cobalt atoms and one nitrosyl ligand, and (f) the  $xz$  plane. Contouring is as in Figure 6.

ligands are much smaller than the  $\pi$  accumulation regions about the nitrosyl ligands in the  $xy$  plane. Additionally, the oval contour about the Co–Co axis in the center of these maps might be mistaken for a region of higher density accumulation at first. However, this oval contour represents a region of lower density accumulation than the accumulation region which surrounds it. Actually, the region about the Co–Co midpoint is a region of almost zero density accumulation indicative of little direct bonding between the two cobalt atoms.

The deformation density maps obtained from the  $140^\circ$  geometry are drastically different from the maps obtained from the  $180^\circ$  geometry. The deformation density maps from the  $140^\circ$  geometry are shown for the RHF wave function in Figure 8a and for the GVB wave function in Figure 8d. Rather than showing the density of two doubly occupied cobalt  $d_x$  orbitals, the  $140^\circ$  maps show two lobes of density accumulation about the Co atoms in the direction from the midpoint of the cyclopentadienyl C–C bond (indicated by a “+” in the maps) toward the projection of the nitrosyl nitrogen atoms in this plane. Almost perpendicular to this accumulation region is a region of density deficit about the cobalt atom pointing toward the coplanar carbon atom of the cyclopentadienyl ligand to a region of density accumulation on the opposite side of the cobalt atom in an area where a Co–Co bent bond might be expected to be. This pattern of density loss near the atomic centers and density gain in the internuclear region is what can be expected from constructive interference between bonding orbitals. Thus, this deformation density map indicates that a direct metal–metal bent bond exists in the RHF wave function of the  $140^\circ$  geometry of  $(\eta^5\text{-C}_5\text{H}_5)_2\text{Co}(\mu\text{-NO})_2$ . The map obtained from the GVB wave function exhibits similar patterns, but the density accumulation due to the metal–metal bent bond is much smaller and the deficit region about the cobalt atoms has become similar to a tilted  $d_x$  orbital.

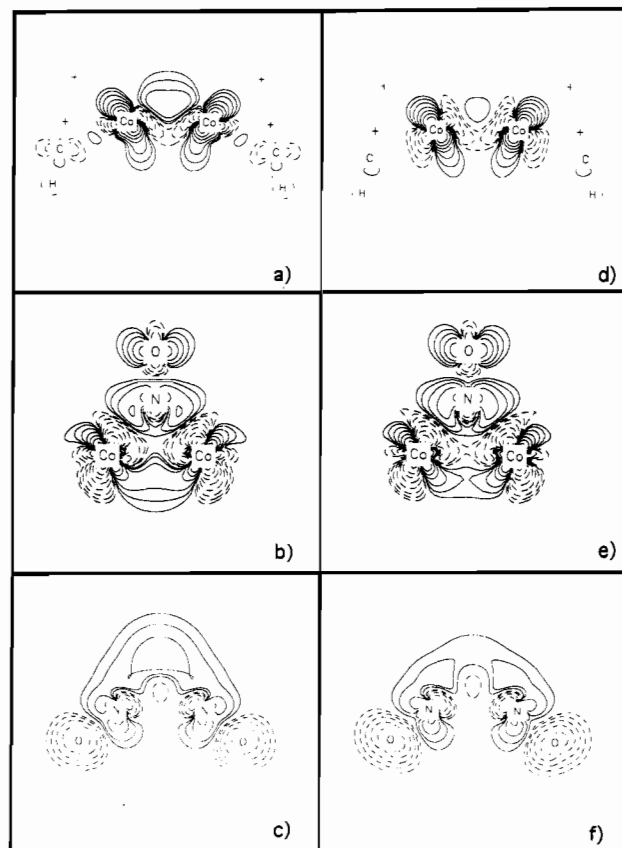


**Figure 9.** Deformation density maps for  $\text{Cp}_2\text{Co}_2(\mu\text{-NO})_2$  in the  $100^\circ$  geometry for the RHF wave function in (a) the  $yz$  plane, (b) the plane containing both cobalt atoms and one nitrosyl ligand, and (c) the  $xz$  plane and for the five-pair GVB wave function in (d) the  $yz$  plane, (e) the plane containing both cobalt atoms and one nitrosyl ligand, and (f) the  $xz$  plane. Contouring is as in Figure 6.

In contrast to the deformation density maps in the  $yz$  plane, the deformation density maps of the  $140^\circ$  geometry in the plane containing one of the nitrosyl ligands and both cobalt atoms, shown for the RHF wave function in Figure 8b and for the GVB wave function in Figure 8e, are quite similar to the maps of the  $180^\circ$  geometry. These maps exhibit large  $\pi$  accumulation and  $\sigma$  loss in the region about the nitrosyl ligand. The accumulation in the  $\pi$  region of the nitrosyl ligand is larger in the GVB map. Both maps exhibit large Co–N bond accumulations which appear as extensions of the nitrosyl's  $\pi$  accumulation regions. Near the cobalt atoms there is a region of density deficit in the direction of the nitrosyl ligands. Perpendicular to the region of density deficit is a region of density accumulation which extends into a region between the two cobalt atoms. Along the Co–Co axis is a region of slight density deficit which becomes less negative as one approaches the Co–Co midpoint. The deformation density maps in the plane containing both nitrosyl ligands, shown for the  $140^\circ$  geometry for the RHF wave function in Figure 8c and for the GVB wave function in Figure 8f. These maps are also very similar to the deformation maps of the planar geometry exhibiting regions of density accumulation in the  $\pi$  region and density deficit in the  $\sigma$  region. The Co–Co bent bond accumulation can clearly be observed in the RHF map. However, in the GVB maps, the accumulation region which might be associated with the Co–Co bent bond might more accurately be described as the superposition of the accumulation regions due to  $\sigma$  donation of the nitrosyl ligands.

The deformation density maps for the  $100^\circ$  geometry (Figure 9) are fairly similar to the maps for the  $140^\circ$  geometry. The region of density accumulation attributed to the Co–Co bent bond has grown larger in the  $100^\circ$  maps. As in the previous pair of maps, the bond accumulation in the GVB map is much smaller than that in the RHF map. The maps in the plane containing



the cobalt atoms and one of the nitrosyl ligands show the features due to strong Co–N bonding through metal to ligand  $\pi$  donation and ligand to metal  $\sigma$  donation as noted in the previous maps. The deformation density maps in the plane containing both nitrosyl ligands exhibit features similar to those in the previous maps with accumulation regions in the nitrosyl  $\pi$  regions and deficit in the nitrosyl  $\sigma$  regions with the  $\pi$  accumulations in this plane being much less than the  $\pi$  accumulations in the plane containing one nitrosyl and the cobalt atoms.

From this series of deformation density maps, the following conclusions can be made. There is no evidence of any direct Co–Co bonding in the 180° geometries. From the patterns in the deformation density maps, it can be observed that the two electrons which could be assigned to the formation of a Co–Co bent bond actually occupy nonbonding orbitals which are perpendicular to the Co–Co axis. This would be consistent with the analysis of the GVB wave function for the 180° geometry, which is suggestive of singlet radical pair of electrons with one electron on each cobalt in the  $d_{z^2}$  orbital of the cobalt atom. As the molecule bends, the maps show some evidence of a direct Co–Co bonding interaction which could be attributed to a Co–Co bent bond. When electron correlation in the form of a one-pair GVB calculation is introduced, the interaction lessens somewhat because of the introduction of substantial Co–Co antibonding character into the wave function. All the maps show features which suggest strong Co–N bonding through metal to ligand  $\pi$  donation and ligand to metal  $\sigma$  donation. Most of the cobalt–nitrosyl interaction occurs in the plane which contains the Co–Co axis, but there is also some metal–ligand interaction in the perpendicular plane.

**Topological Analysis.** A topological analysis of the electron density has a particular advantage over deformation density studies due to the fact that it is not dependent on any arbitrary reference point such as a promolecule. A topological analysis of the charge density should lead to a less ambiguous interpretation of the existence of a bond between two adjacent atoms. A necessary requirement for the existence of a bond between adjacent atoms is that there be an atomic interaction line connecting the two atoms called a bond path. On this bond path, the charge density must be a maximum in all directions perpendicular to the bond path. According to this analysis, the “boundary” between two atoms is notated by a zero-flux surface between them. Where this zero-flux surface crosses the bond path, a (3,–1) critical point exists. Therefore, a quick method of determining whether two adjacent atoms are bonded is to locate a (3,–1) critical point between them.

In a previous study on  $\text{Co}_2(\text{CO})_8$ ,<sup>26</sup> the topology of the theoretical charge density possessed no bond path connecting the two cobalt atoms, which is an indication of no direct Co–Co bonding. This was in contrast to the deformation density results which suggested some constructive interference between the two cobalt atoms. However, the Co–Co separation in  $\text{Co}_2(\text{CO})_8$  is about 0.2 Å longer than the same Co–Co distance in compound 1. When the Co–Co separation was shortened to the cobalt–cobalt separation found for 1, a bond path connecting the cobalt atoms as well as the corresponding (3,–1) critical point was found which is indicative of a direct Co–Co bond.

The critical points associated with the  $\text{Co}_2(\mu\text{-NO})_2$  portion of compound 1 for the 100, 140, and 180° geometries for the RHF density and the one-pair GVB density are listed in Table IV. Along with the position of the critical points are listed the values of the density  $\rho$ , the Laplacian  $\nabla^2\rho$ , and the ellipticity  $\epsilon$  of the critical points. The values of  $\rho$  and  $\nabla^2\rho$  are indicators of the relative strength and nature of the bond between the connecting atoms, whereas the ellipticity is a measure of the nonsphericity of the charge about the critical point.

The critical point found between the cobalt atoms will also be analyzed further by its eigenvalues. The eigenvalues of the critical point are the value of the second derivative in the three directions which are associated with the critical point. One of these directions is the direction along the atom–atom interaction line, and its

**Table IV.** Critical Points Associated with the  $\text{Co}_2(\mu\text{-NO})_2$  Ring RHF and GVB Wave Functions of 100°, 140°, and Planar Geometries of 1

100° Geometry			
atom	x	y	z
Co	0.0000	±2.2393	0.1906
N	±2.0093	0.0000	–1.4954
O	±3.7276	0.0000	–2.9372

Critical Points <sup>a</sup>							
atoms	x	y	z	$\rho$	$\nabla^2\rho$	$\epsilon$	type
Co–Co (GVB)	0.0000	0.0000	0.0829	0.0511	0.3505	38.2766	(3,–1)
Co–N (GVB)	±1.4414	±1.3094	0.0331	0.1328	0.5758	0.1768	(3,–1)
N–O (GVB)	±0.9919	±1.0876	–0.6511	0.1360	0.6564	0.1717	(3,–1)
Co <sub>2</sub> N (GVB)	±3.6028	0.0000	0.0012	0.4843	–1.2867	0.0273	(3,–1)
Co <sub>2</sub> N <sub>2</sub> (GVB)	±2.7747	0.0000	–2.1150	0.4779	–1.1994	0.0558	(3,–1)
Co <sub>2</sub> N (GVB)	±0.3285	0.0000	0.0952	0.0574	0.3170		(3,+1)
CoN <sub>2</sub> (GVB)	0.0000	0.0000	–1.2793	0.0597	0.3180		(3,+1)
Co <sub>2</sub> N <sub>2</sub> (GVB)	0.0000	0.0000	–0.5705	0.0526	0.4056		(3,+3)
Co <sub>2</sub> N <sub>2</sub> (GVB)	0.0000	0.0000	–1.2337	0.0571	0.3159		(3,+1)

140° Geometry			
atom	x	y	z
Co	0.0000	±2.2393	0.1100
N	±2.4648	0.0000	–0.7871
O	±4.5726	0.0000	–1.5543

Critical Points <sup>a</sup>							
atoms	x	y	z	$\rho$	$\nabla^2\rho$	$\epsilon$	type
Co–Co (GVB)	0.0000	0.0000	0.2194	0.0535	0.3149	7.9660	(3,–1)
Co–N (GVB)	±1.2953	±1.2450	–0.2596	0.1319	0.6899	0.3766	(3,–1)
N–O (GVB)	±1.2617	±1.1930	–0.2280	0.1321	0.7236	0.5186	(3,–1)
Co <sub>2</sub> N (GVB)	±3.3804	0.0000	–1.1185	0.4821	–1.1186	0.0341	(3,–1)
Co <sub>2</sub> N <sub>2</sub> (GVB)	±3.3678	0.0000	–1.1152	0.4768	–1.1743	0.0698	(3,–1)
Co <sub>2</sub> N (GVB)	±0.1628	0.0000	0.1967	0.0534	0.3191		(3,+1)
Co <sub>2</sub> N <sub>2</sub> (GVB)	0.0000	0.0000	–0.0554	0.0496	0.3943		(3,+1)

Planar Geometry			
atom	x	y	z
Co	0.0000	±2.2393	0.0000
N	±2.6229	0.0000	0.0000
O	±4.8660	0.0000	0.0000

Critical Points <sup>a</sup>							
atoms	x	y	z	$\rho$	$\nabla^2\rho$	$\epsilon$	type
Co–N (GVB)	±1.4414	±1.3094	0.0339	0.1328	0.5758	0.1768	(3,–1)
N–O (GVB)	±1.3775	±1.2952	0.0243	0.1300	0.7429	0.4532	(3,–1)
Co <sub>2</sub> N (GVB)	±3.6028	0.0000	0.0012	0.4843	–1.2862	0.0273	(3,–1)
Co <sub>2</sub> N <sub>2</sub> (GVB)	±3.5838	0.0000	0.0000	0.4759	–1.1720	0.0831	(3,–1)
Co <sub>2</sub> N <sub>2</sub> (GVB)	0.0000	0.0000	0.0829	0.0829	0.3503		(3,+1)
Co <sub>2</sub> N <sub>2</sub> (GVB)	0.0000	0.0000	–0.0554	0.0496	0.3943		(3,+1)

<sup>a</sup> The first line shows the critical point associated with the particular region for the RHF wave function, and the second line shows the critical point associated for the same region for the GVB wave function. A line with no entries means that no critical point exists for that particular region for that wave function.

eigenvalue,  $\lambda_3$ , is usually large and positive. The remaining two directions are perpendicular to the atom–atom interaction lines, and these eigenvalues are normally notated as  $\lambda_1$  and  $\lambda_2$ . By convention, the absolute value of  $\lambda_2$  is always larger than that of  $\lambda_1$ . When both perpendicular eigenvalues are negative, a (3,–1) bond critical point exists. When one of the perpendicular eigenvalues is positive, a (3,+1) ring critical point exists.

For the 180° geometry, we find all of the expected features associated with the four Co–N bonds and the two N–O bonds in the  $\text{Co}_2(\mu\text{-NO})_2$  ring. The bond paths associated with the Co–N bonds lie slightly outside of the ring formed by drawing straight lines from all of the four atoms in the  $\text{Co}_2\text{N}_2$  ring, indicative of some ring strain in this bonding arrangement. The (3,–1) critical

point lying on the Co–N bond path lies slightly closer to the cobalt atom and has a large ellipticity indicative of differential  $\pi$  character in this bond. There is also a bond path connecting the nitrogen and oxygen atoms in a nitrosyl molecule. The (3,–1) critical point on the N–O bond path lies closer to the nitrogen atom and possesses a very small ellipticity which is typical for triply bonded molecule. The only critical point that can be found between the cobalt atoms in the 180° geometry is a (3,+1) ring critical point which can be associated with the  $\text{Co}_2\text{N}_2$  ring. The (3,+1) ring critical point lies approximately at the midpoint of the Co–Co axis. If the values of  $\rho$  and  $\nabla^2\rho$  are examined for this ring critical point, it can be noted that there is very little charge density present at the ring critical point. The conclusion that can be drawn from the lack of a bond path connecting the two cobalt atoms is that there is no direct cobalt–cobalt bonding in the wave function for the 180° geometry. The GVB wave function for the 180° geometry yields the same topology of the charge density as the RHF wave function.

Upon folding of the planar structure of **1**, the topology of the charge density changes drastically as shown in the list of critical points for the 140° geometry. The topology from the RHF density yields a bond path connecting the two cobalt atoms. The (3,–1) critical point between the two cobalt atoms lies equidistant between the cobalt atoms 0.109 atomic units off the Co–Co axis in the direction opposite the nitrosyls. This result is what would be expected from a Co–Co bent bond. The bond paths associated with the remainder of the  $\text{Co}_2(\mu\text{-NO})_2$  ring are very similar to those found in the 180° geometry and will not be discussed further. When one compares the (3,–1) critical points in the  $\text{Co}_2(\mu\text{-NO})_2$  ring, it can be noted that the value of  $\rho$  for the Co–Co (3,–1) critical point is significantly smaller than the same values for the other (3,–1) critical points in the ring. This result is indicative of the weaker nature of the Co–Co bond when compared to the other bonds in the molecule. Additionally, if one examines the perpendicular eigenvalues of the Co–Co (3,–1) critical point of –0.0462 (*z* direction) and –0.0052 (*x* direction) and compares them to the perpendicular eigenvalues of the remaining (3,–1) critical points, it can be noted that those of the Co–Co (3,–1) critical point are extremely small. This is an indication of the flat nature of the charge density about this critical point. The remainder of the critical points associated with the  $\text{Co}_2\text{N}_2$  ring are two (3,+1) ring critical points which are within the rings formed by the Co–Co bond path and the Co–N paths. The (3,+1) ring critical points are located fairly close to the (3,–1) critical point between the cobalt atoms.

The topology of the electron density changes when correlation is added to the 140° geometry as in the GVB wave function. For the GVB density, the bond path which connected the cobalt atoms in the RHF density disappears. Now the topology resembles that of the 180° geometry, where there is a single (3,+1) ring critical point between the cobalt atoms. If one compares the values of  $\rho$  of this (3,+1) critical point to the (3,–1) critical point from the RHF density, it can be noted that the density at the critical point does not change much upon the addition of correlation. In fact, the major change that occurs in the GVB density is that one of the perpendicular eigenvalues of the critical point between the cobalt atoms changes sign from –0.0052 to 0.02875. This change in sign turns the (3,–1) bond critical point into a (3,+1) ring critical point. However, the change is a very slight change indeed and is another indication of the flat nature of the charge density in the internuclear region between the cobalts. The flat nature of the topology of the charge density and the small value of the charge density leads to the conclusion that if a direct metal–metal bond exists in this molecule, it would be very weak indeed due to the lack of electron density.

As the folding of compound **1** increases, the (3,–1) critical point which appears in the RHF density between the two cobalt atoms increase its  $\rho$  value and the perpendicular eigenvalues become increasingly more negative. However, as for the larger angles in the other cases, this (3,–1) critical point disappears in

the GVB density. There are added features in the topology of the charge density of the 100° geometry. The RHF density shows some interaction between the nitrogen atoms of the two nitrosyl ligands with the appearance of a (3,+1) critical point between the nitrogen atoms and a (3,+3) cage critical point inside the  $\text{Co}_2\text{N}_2$  “cage.”

These results might suggest that the Co–Co bent bond, which disappears upon the addition of correlation, may be an artifact of the RHF wave function. However, it is also an indication of the definite nature of the topological analysis. In this analysis, a bond either exists between two atoms or it does not. There is not a gradual change between bonded and nonbonded states. Deformation density studies show a more gradual transition from nonbonded Co atoms at 180° to weakly bonded Co atoms between 140 and 100°. Even though the deformation density study suggested some constructive interference between the cobalts for the bent geometries of **1**, even for the GVB wave function, the topological analysis is dominated by the contraction of charge density toward the cobalt atoms in the GVB wave function and whatever constructive interference exists is not enough to produce a bond critical point in the GVB calculations.

## Conclusions

From the results of our *ab initio* molecular orbital calculations, it can be concluded that the more stable geometry of  $(\eta^5\text{-C}_5\text{H}_5)_2\text{-Co}_2(\mu\text{-NO})_2$  is bent, or folded, along the Co–Co axis. This result is in agreement with spectroscopic observations on this compound but not with the X-ray structure. Additionally, our calculations indicate that for the bent geometries of  $(\eta^5\text{-C}_5\text{H}_5)_2\text{Co}_2(\mu\text{-NO})_2$ , the electronic ground state is definitely a singlet state. The lack of experimental observation of a low-lying triplet state is another indication that this compound is not planar.

The question of a direct metal–metal interaction between the cobalt atoms in this compound really has not been answered definitely by this study, and it seems to depend upon whether the molecule is bent or planar. At this point, all analyses agree that the direct Co–Co “interaction” is weak and near the “borderline” between bonding and nonbonding. A reexamination of the structure by X-ray diffraction to establish the correct Co–Co bond length would be helpful to further investigation of this interesting class of compounds. For the more stable bent geometries of this molecule, the deformation density study indicates that there is a small amount of constructive interference between the cobalts in the region associated with a bent Co–Co bond. Whether this can be equated with a direct Co–Co bond is really a question of what one defines as a chemical bond. The topological analysis, which has an unambiguous definition, suggests that a Co–Co bent bond is an artifact of the RHF wave function which disappears upon the addition of electron correlation. However, analysis of the GVB pair orbitals of the GVB wave function indicates that there is some degree of covalent bonding between the cobalt atoms in the bent geometries. Furthermore, the bond critical point which disappeared with the GVB wave function might reappear with improvement in basis set and electron correlation. For the 180° geometry, there is definitely no direct Co–Co interactions and the electronic ground state of the molecule possesses a radical singlet pair of electrons, which occupy the nonbonding  $d_{z^2}$  orbitals on each cobalt atom and indicate a low-lying triplet state.

**Acknowledgment.** The authors acknowledge the support of the National Science Foundation (Grant CHE 91-13634).